International Journal of Concrete Structures and Materials
Vol.11, No.3, pp.541–555, September 2017
DOI 10.1007/s40069-017-0204-9
ISSN 1976-0485 / eISSN 2234-1315

Effect of Scoria on Various Specific Aspects of Lightweight Concrete

Eddie Franck Rajaonarison[1)], Alexandre Gacoin[2)], Roger Randrianja[1)], Velomanantsoa Gabriely Ranaivoniarivo[1)], and Bam Haja Nirina Razafindrabe[3),*]

(Received September 14, 2015, Accepted May 15, 2017, Published online September 18, 2017)

Abstract: Experimental research on the technical characteristics of lightweight concretes incorporating scoria was conducted. The objective of this research is to investigate the feasibility and effectiveness of the use of scoria, in lightweight concretes. Coarse scoria of 5/10 and 10/20 mm were used. A portion of the aggregate mixtures had an average particle size ≤100 μm. Scorias are often used as the constituents of structural concrete and insulating materials. The usability of the concretes tested in this study broadens as the porosity of the mixtures decreased and the cement dosage increased. According to the cement dosage and frequency types, the absorption coefficients of concretes ranged from 0.14 to 0.47. A compressive strength of 19 MPa corresponded to a density of 1800 kg/m^3; compressive strengths from 10 to 18 MPa mapped to densities ranging from 1300 to 1700 kg/m^3. The thermal conductivity of mixed concretes without scoria reached a maximum value of 0.268 W/m K. The thermal conductivity values of the concretes mixed without sand were below 0.403 W/m K. As sand content increased, the conductivity evolved from 0.565 to 0.657 W/m K. Freeze–thaw stability tests were conducted for 400 cycles or until specimens deteriorated. The experimental results helped in determining the optimum mixing conditions for the inclusion of scoria in cement to produce lightweight concretes.

Keywords: scoria, lightweight concrete, thermal and acoustic properties.

1. Introduction

Structural lightweight aggregate concrete is made with lightweight aggregates, as defined in ASTM C330. This variety of concrete has a minimum 28-day compressive strength of 17 MPa, an equilibrium density between 1120 and 1920 kg/m^3, and a composition entirely of lightweight and normal-density aggregate materials (ACI 2003). Relatively low-density aggregates can be obtained by substituting classical aggregates of sand and pea gravel with artificially lighter aggregates, such as expanded polystyrene beads (Chen and Liu 2004; Khedari et al. 2003). Experimental works have shown that the characteristics of the aggregates are highly active in lightweight concretes, dictating the good mechanical, thermal, and acoustical performance of the final concrete (Lotfy et al. 2015; de Sensale and Goncalves 2014; Chi et al. 2003).

Some modified types of concrete under thermomechanical loadings have been developed (De Sa et al. 2006; Burlion et al. 2005). The selection of materials is essential from the acoustical point of view. Materials can be classified into three main categories: transmission, reflection, and absorption. Good knowledge of these factors will help specialists to develop and implement sound-absorbing walls, which offer the best value for money with high acoustical performance levels. A micro perforated panel (MPP) was proposed (Maa 2007) as a next-generation alternative for porous sound-absorbing material, which has various issues related to health, hygienic, and environmental aspects. Many studies on MPPs have since been conducted (Kang and Brocklesby 2005; Asdrubali and Pispola 2007). Some studies on plate absorption were conducted. Others were more focused on radiation (Ruzzene 2004), and in particular, the vibration and radiation of sound from sandwich beams utilizing an MPP.

Moreover, salt scaling is defined as the "superficial damage caused by freezing a saline solution on the surface of a concrete body" (Valenza II and Scherer 2007). Concrete scaling is caused by the formation of an ice lens, which induces constraints on the material periphery. The damage from the frost, and from scaling in particular (Valenza II and Scherer 2007), most frequently occurs in the wet regions of concrete in which the material surface is water-saturated under rigorous wintry conditions of severe frost.

Several researchers have investigated the effects of scorias as replacements for cement, namely with respect to the mortar

[1)]Sciences of Materials and Metallurgy, Ecole Supérieure Polytechnique, University of Antananarivo, 101 Antananarivo, Madagascar.

[2)]Search Group on Sciences for the Engineers, GRESPI/Thermomécanique, University of Reims Champagne-Ardennes, Campus du Moulin de la Housse - BP 1039, 51687 Reims Cedex 2, France.

[3)]Faculty of Agriculture, University of the Ryukyus, 1 Senbaru, Nishihara, Okinawa 903-0213, Japan.
*Corresponding Author;
E-mail: bamrazaf@agr.u-ryukyu.ac.jp

Copyright © The Author(s) 2017. This article is an open access publication

toughness, cement fraction (Al-Swaidani and Aliyan 2015; Bondar 2015; Lotfy et al. 2015; Ghrici et al. 2007; Rabehi et al. 2014), the fabrication of granulate forms for lightweight concretes (Mouli and Khelafi 2008), and thermal activation (Ezziane et al. 2007). Most studies have shown that scorias are economically sound and ecologically friendly building materials (Vlček et al. 2014). Scoria, as lightweight aggregate, has been used in concrete to produce structural lightweight concrete, especially in Turkey (Yaşar et al. 2004). However, most of these works have not included the simultaneous research on the mechanical, thermal, and acoustic characteristics of the building materials incorporating scorias.

In this study, the ability of scoria to replace all aggregates is emphasized. The objective of this research is to investigate the feasibility and effectiveness of using scorias in lightweight concretes.

In the present work, the mechanical, thermal, and acoustical behaviors of these scorias used as a base in concrete were studied. These materials were simultaneously considered according to two characteristic relations: mechanical/thermal and mechanical/acoustical. The second motivation arises from a desire to better understand the thermo-acoustic mechanisms at stake. The aptitude of scoria concretes to resist damage by freeze–thaw cycles was particularly of focus. In short, in the framework of this experimental research, the continuity of the works carried out by predecessors in this field is a synonym of process diversity because a common base or reference material uniting this work with those in the past is scoria and its different compositions.

2. Materials and Methods

2.1 Materials

The following materials were used to produce different concretes. The cement used during our experiments is type I (ASTM C150 2009). The physical properties and chemical composition of this cement are listed in Table 1. Potable water meeting the requirements of ASTM C 1602-06 (2009) was used to mix the concretes, and saturated lime-water (Bediako et al. 2015) was used to cure the specimens. The scoria extraction site, is located in Antsirabe, 167 km away in the southern part of Antananarivo, capital of Madagascar. The scoria in this geographical structure is better preserved compared with that of the volcanic cones in Madagascar (UNESCO 1995). Its main mass, which has not been estimated, is formed by projection products, among which scorias widely dominate.

The scoria samples were processed by identification and characterization tests. Chemical analyses of samples of the powdered scoria were performed. The method of powder X-ray diffraction was used on the samples and required a monochromatic X-ray beam. The powder was examined by a Siemens D500 diffractometer using monochromatic CuKa radiation with a wavelength $\lambda = 1.7903$ Å at a voltage of 40 kV and a current of 30 mA. The obtained results are shown in Fig. 1.

Table 2 summarizes the main characteristics of the scoria samples used for this study while Table 3 shows the results of the chemical and mineralogical analyses for these samples. The dominant minerals are nepheline, orthose and

Table 1 Physical and chemical properties of cement.

Specific gravity (g/cm^3)		3.15	ASTM C 188-03
Specific surface (cm^2/g)		3897	ASTM C 204-05
Setting time initial (min)		30	ASTM C 191-04
Compressive strength (MPa)			
	1 days	10.4	
	3 days	21.3	
	7 days	33.5	
	28 days	43.6	
Chemical composition, % by mass			
	SiO_2	20.5	
	Al_2O_3	4.52	
	Fe_2O_3	2.71	
	CaO	63.93	
	MgO	2.39	
	K_2O	1.01	
	SO_3	3.3	
	Na_2O	0.19	
	LOI	0.97	

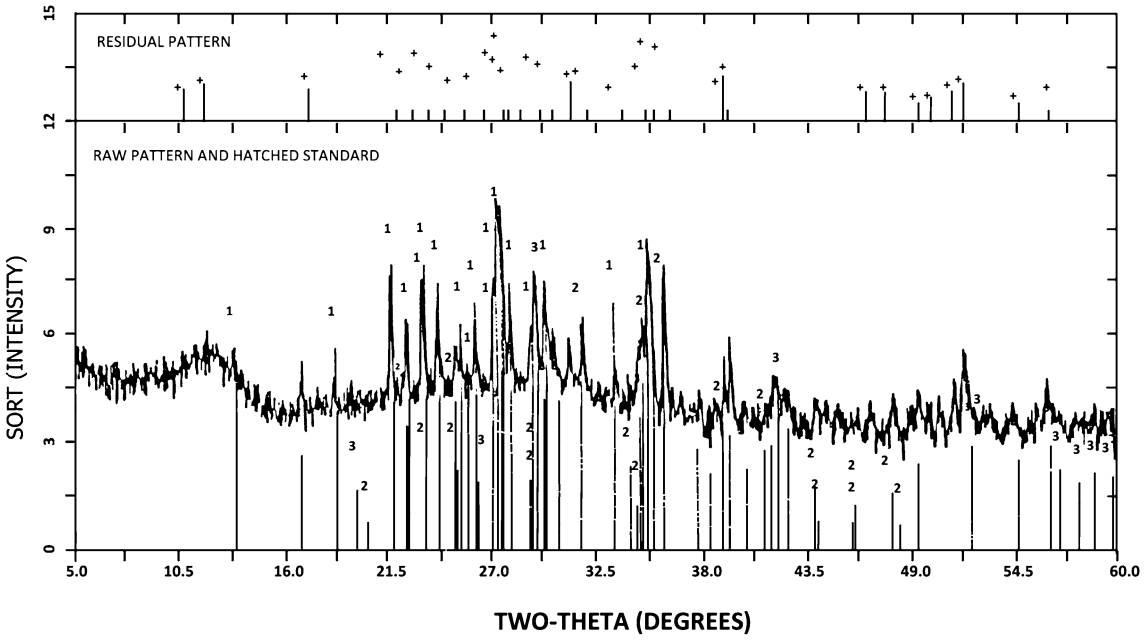

	FRACT	STANDARD		I/ICOR	FOM	
1	45	9.0465	(CA. NA) (SI. AL) 40	1.0	0.575	Calcic plagioclase
2	28	21.1257	(MGO. 6FEO. 4) 2SIO	1.0	0.385	Olivine (rich in iron)
3	26	24.0202	CA (MG. AL. FE) SI2O	1.2	****	pyroxen

Fig. 1 X-ray diffraction analysis.

Table 2 Scoria used in the study.

Color	Form	State of surface	Structure	Appellation
Purplish-blue black	Scoriaceous	Very rough	Porous	scorias

magnetite. Furthermore, the secondary minerals are diopside and foresterite.

The sand used in this study comes from Antananarivo, Madagascar. It is siliceous. Its rolled grains, round form, and smooth surface are characterized by their quality. The average specific mass is $\gamma s = 2.66$ kg/l for the tested samples. The tested apparent density (average value) is $\gamma s = 1.52$ kg/l. As for the sand used in this study, its porosity is PS = 42, 86% and the sand equivalent is ES = 72%.

The ASTM C618 (ASTM C 618 2001) standard was used when setting the characteristics of the scoria. The average values of silica, alumina, and ferric oxide in the scoria are within 43–55, 12–24, and 8–20%, respectively. These ranges serve to ensure cohesion between the chemical elements, specifically indicating that substance cohesion plays an essential role in this material property.

Scoria samples were composed of alumina, silica, and ferric oxide in compliance with the characteristic limits set by NFP 18 308. The alkali values are presented in equivalent values of Na_2O, a metric commonly used by cement workers (UCGCT 2009; Beycioğlu et al. 2010).

A careful testing of the apparent and absolute densities of the aggregate as well as on water content in natural state of the scoria was conducted. The average tested apparent density of the S1 aggregates is 1.47 T/m^3. Its average real density and water content are respectively 2.89 and 6%. The fine phases used in some of the mixtures were 100-µm constituents taken from Antsirabe milled scorias. The material finer than 75 µm, which represents the dust in the scoria, was tested according to ASTM C-117 (ASTM C117 2004). The particle size distribution of the aggregates is shown in Fig. 2. The amount of dust was found to increase near the ground surface and decrease with the depth. The material with an average density of 1.15, taken from the main pit of the quarry showed an average proportion of material finer than 75 µm, ranging between 0.4 and 0.6%. The investigation indicated that a voluminous deposit of scoria located at a greater depth satisfied the ASTM C-33 requirements for both the range and average proportion of material finer than 75 µm. Photographs of the scoria samples are shown in Fig. 3.

An experimental study is imperative for a better understanding of the interaction between fine constituents and coarse aggregates. Some authors (Rossignolo et al. 2003; Beaucour et al. 2003) have studied the behavior of granular mixtures to obtain an optimal concrete formulation. For ternary mixtures, the interactions among the sand, fines, and gravels need to be analyzed. Binary mixtures of fines and gravels can confirm the behavior of these interactions.

Table 3 Chemical composition of scoria.

Elements	%
SiO_2	44.63
Al_2O_3	13.04
Fe_2O_3	12.48
CaO	12.08
MgO	09.56
K_2O	01.33
SO_3	00.02
TiO_2	02.29
MnO	00.21
Na_2O	02.40
Cr_2O_3	00.11
P_2O_5	00.71
LOI	01.15
Total	100.01

2.2 Binary and Ternary Mixtures

From theoretical and experimental points of view, some authors (Al-Chaar et al. 2011; Parhizkar et al. 2010) have carried out works on the scoria behavior. In this study, an experimental protocol was set up to determine the composition of scoria concretes.

Regarding ordinary concretes, the main objective is to make and obtain concretes with minimum porosity. In fact, these concretes have the best mechanical resistances. For lightweight aggregate concretes that differ slightly from ordinary concretes, the objective is to obtain mixture rules compatible with the composition of ordinary concretes, a low density, and good physical and mechanical characteristics.

However, there is an incompatibility between these characteristics, which does not enable the optimization of the mixture. If the thermal and acoustic resistances increase, the mechanical resistance decreases. The linear variation rule of the theoretical void ratio is governed by the mixture rule of two aggregates, expressed as follows (Bhattacharjee 2014):

(a) Pozzolan quarry. **(b)**gravel pozzolan. **(c)**fines pozzolan.

Fig. 3 Scoria samples.

$$e = \alpha V_{abs} + \beta \quad (1)$$

where e is the void ratio; α and β are the coefficients of the void ratio and the form of the grains, respectively, and V_{abs} is the absolute volume of aggregates in 1 m^3 of concrete.

Grain forms appeared to have an influence on the void ratio, corroborated with the effects of the plates and the interference of the aggregates. Thus, an experimental study is imperative to achieve greater understanding of the interaction between fine and coarser aggregates. This behavior can be observed for a scoriaceous form such as coarse scorias. For ternary mixtures (sand river + scoria + cement), the interactions between the sands, fillers, and gravels have to be analyzed. Typically, fillers and gravels behave as binary mixtures (scoria + cement).

Ternary mixtures require experimental study to understand the influence of the variations in the void ratio. In the tested binary mixtures, the actual volume of the coarse scoria (V_r) was constant for the compositions categorized by specimens bc1–bc6. A progressive reduction in the cement dosage was conducted with respect to the void ratio results. The quantities of fines used were calculated to account for the total value of the absolute volume of the mixture in cement substitution, which implies that fine scoria can be surely used as an additive or substitute for cement in concrete mixtures (Al-Chaar et al. 2011).

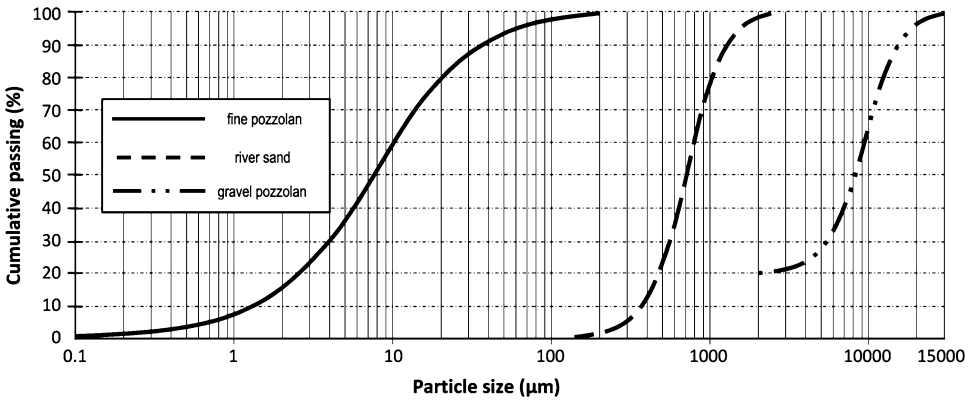

Fig. 2 Particle size distribution of aggregates.

Table 4 Binary concretes composition.

Denomination	Bc1	Bc2	Bc3	Bc4	Bc5	Bc6	Bc7	Bc8
V_c (kg/m^3)	146	140	122	120	115	85	134	120
V_f (kg/m^3)	182	222	139	77	00	00	254	287
V_{ab} (kg/m^3)	301	301	301	301	301	301	243	188
V_r (kg/m^3)	537	537	537	537	537	537	433	335
W (kg/m^3)	170	170	170	170	170	170	170	170
Density (kg/m^3)	1715	1720	1625	1345	1260	1200	1715	1730

V_c volume of cement, V_f volume of fines, V_{ab} absolute volume of the scoria, V_r real volume of the scoria, W water in kg/m^3.

It is noted that Vr was reduced in order to increase the significance of the void ratio for specimens bc7 and bc8. Table 4 presents the mixture compositions used this study.

For ternary mixtures, the experimental volumetric method was conducted according to ASTM C33 (ASTM C 33-03 2003). For this, concerning the solid constituent dosages, coarse aggregates were categorized on the basis of the real volume of the solid after presoaking. The aggregates included coarse scoria pea gravels to the 5/10 series. Ordinary sand was used. The various concrete compositions are listed in Table 5. For series A, B, and C, more sand was added progressively.

For series A, fines were not used, and the quantity of pea gravel was the same for specimen number 1, 2, and 3. During the experiments, the sand quantity and cement dosage were increased. For specimen no. 4, the amount of pea gravel was reduced while the sand quantity was increased. The cement dosages are listed in Table 7. The choice of these compositions is based on previous works, as reported by Durán-Herrera et al. (2011) for an experimental reason.

For series B, the fine phase in specimen no. 4 and 5 was not used. In this series, the amount of sand was increased, and the quantities of pea gravel and cement were progressively decreased. Similar results can be obtained for a binary concrete belonging to the semicavernous series, where the fine aggregates have been removed.

For series C, the cement dosage was fixed at 450 kg/m^3 for specimens 1–4 while progressively increasing the amount of sand. For batch no. 5, the cement dosage was reduced to 350 kg/m^3 with a sequence of reductions in the amount of fines in order to know the influence of the cement dosage exactly.

Calculations of the amount of aggregate used allowed us to define the mixtures according to the desired concrete as either voluminous or not. In this study, the apparent density was determined by finding the mass of a hardened 4 cm × 4 cm × 16 cm parallelepiped sample with a KERN Pit 720-3A precision weighting balance (the analysis balances KERN, with this measurement principle, are branded "Single-Cell Technology": SC TECH).

The choice of parametric formulations was made according to the influence of the aggregate nature and volumetric concentration on the mechanical, thermal, and acoustical behavior of lightweight scoria concrete.

Scoria affects the workability of fresh scoria concretes. Different mixes were studied by conducting slump tests, as per ASTM C 143 (ASTM C 143 2014). The study demonstrates that there is no significant variation in the slump loss of scoria concrete and the control mix. The initial slump of all mixes was within the range of 105 ± 15 mm.

In this study, various molds were used according to the tests being conducted. For mechanical testing, cylindrical paperboard molds were used (with a height of 320 mm and a diameter of 160 mm). For thermal testing, slabs measuring 27 cm on a side and 5 cm in thickness were made. For acoustical testing, prisms with heights of 10, 20, or 30 cm with a constant side length of 8.5 cm were used. The sample size for each test type was determined by the fixed dimensions of the measurement devices. The following section describes the mechanical characterization of the scoria lightweight concretes.

2.3 Mechanical Characterization

The mechanical characteristics of concretes are commonly analyzed and better known compared to other characteristics because of the very important structural role of the materials in civil engineering works. The mechanical properties of concretes are frequently given at a curing age of 28 days. The measurements carried out in this study were performed following the ASTM C39 Standard Test Method for the compressive strength of cylinder concrete specimens.

2.4 Thermophysical Characterization

Measurement of the thermal conductivity of concretes is necessary in order to define the capacity for thermal insulation by the materials.

To measure the thermophysical characteristics, our samples were dried in an oven at a temperature of 50 °C. A unidirectional thermal flow traveled through the samples (E), which were placed between cold isothermal and constant heat flux sources. Therefore, the thermal gradient that evolved between these two faces was measured. Once the steady state was established, the apparent thermal conductivity (Bessenouci et al. 2011) could be expressed as

$$\lambda a = \frac{e}{S\Delta T}(q + C\Delta T') \tag{2}$$

Table 5 Ternary concretes composition.

Name	A			B					C				
Specimens no	1	2	3	4	1	2	3	4	5	1	2	3	4	5
Dosage (kg/m^3)	250	350	350	300	450	425	400	350	450	450	450	450	450	350
Sandriver	69	105	162	231	72	191	252	292	332	71	139	237	291	361
Cement	81	115	124	92	147	132	132	116	115	137	136	123	114	111
Fines	00	00	00	00	50	34	13	00	00	156	136	98	110	47
Water	120	160	160	120	175	175	170	155	160	216	221	187	136	187
Pea gravel	537	537	537	493	537	469	384	357	300	465	401	332	231	261
Density (kg/m^3)	1286	1330	1400	1396	1463	1522	1544	1690	1748	1732	1747	1789	1780	1800

where λa is the apparent thermal conductivity, C is the heat loss coefficient (W/C), e is the sample thickness (m), q is the heat flux (W), S is the sample surface area (m^2), ΔT is the thermal gradient between the hot and cold faces of the samples (°C), and $\Delta T'$ is the thermal gradient between the atmospheres outside and inside the oven (°C).

The thermal conditions of the temperature and temperature gradients and the thermal properties of the conductivity, density, and composition of the concrete directly influence the insulating capacity of the concrete. The following test allowed the measurement of the influence of the physical parameters such as the porosity and permeability on the ability of concrete to withstand to freeze–thaw cycles.

2.5 Freeze–Thaw Cycles

Several studies on the frost behavior of concretes have been undertaken. Works on this subject have been published (Hamoushet al., Hamoush et al. 2011; Valenza II and Scherer 2007). The mechanisms linked with crystal formation (Coussy and Fen-Chong 2005; Coussy and Monteiro 2007) or directly applied to materials frozen on a cement basis (particularly in the presence of salts) (Penttala 2006) are the most frequently investigated.

In this study, the influence of ice on the mechanisms of transfer and the microstructural characteristics of lightweight scoria concretes were analyzed. NFP 18-424 was used (Bodet 2014), from which the North American ASTM standard C666/C666M (ASTM standard C666/C666M-03 ASTM Standard 2008) experimental works and tests follow, as well as NF EN 206-1 (Norme NF EN 206-1 2004). For each concrete formulation, three 100 mm × 100 mm × 400 mm prisms were made. Freeze–thaw cycle was increased, and the time for a rise and drop in temperature was reduced to 3 h. A freeze–thaw cycle was performed under water saturation conditions; with thermal cycling, a freeze level of approximately −15 °C was reached in over 2 h, the thaw level to approximately +6 °C occurred over 1 h, and the total cycle duration was 3 h, allowing us to carry out eight cycles per day.

2.6 Frost Plus Deicing Agents

Most salt scaling experiments follow the guidelines in ASTM C672 (ASTM Standard C672 1992). This method consists of confining a pool of a 3-wt% NaCl solution with a depth of 6 mm on the surface of a concrete slab with a thickness of ≥75 mm. Specimens were then placed in a freezer for 16–18 h at a temperature of −17.8 ± 2.8 °C. The samples were then removed and allowed to thaw at 23 ± 3 °C for 6–8 h. At the end of five freeze–thaw cycles, the solution was rinsed off, and the slabs were visually examined. The test ended after 50 freeze–thaw cycles. During visual examination, the specimens were rated on a scale of 0–5, with 0 indicating no scaling and 5 denoting severe scaling.

In addition to ASTM C672, XPP18-420 (French Standard) (XPP 18 420 1995) was also used. This scaling test consisted of submerging test tubes of concrete in the NaCl solution for

24 h of 56 consecutive freeze–thaw cycles between +20 and −20 °C. For each measurement (after each of the first seven cycles as well as after the end of all 56 cycles), the test tubes were brushed, and the loosened particles were collected and washed. They were dried in a stove at a temperature of 105 ± 5 °C overnight and then weighed in order to determine the dried mass. The NaCl solution was then renewed, and the test tube was placed back inside. The cumulated mass of the particles detached from the test tube surface, called the scaling cumulated mass, was thus calculated according to the cycle number.

The hardness of the concrete materials submitted to freeze–thaw cycles is strongly influenced by the nature of the materials. This was characterized by the porosity of the concrete in accordance with conditions to the limits previously described. Materials with a high porosity allow us to measure the sound absorption coefficient and acoustical properties of scoria concretes.

2.7 Acoustical Characterization

Measurements of the reverberation time were recorded, and calculations of the absorption coefficient were obtained by using the Sabine formula; the calculations were based on the measured reverberation times. The measurement were performed using a reverberation room, a 2260 Bruel and Kjaer sound level meter with a 4189 Bruel and Kjaer 1/2″ microphone, and an omnidirectional sound source (4296 Bruel and Kjaer). Spatial averaging was accomplished using nine ranks of microphone positions located at least 1.6 m away from each other. The measurements were performed following ISO 354 (ISO 2003) (ISO 354 2003).

Shock tests were performed according to the following operating procedure: a rectangular concrete plate having a length of 20 cm, a width of 10 cm, and a thickness of 8.5 cm was restrained at one area and excited by an impulse-force hammer to produce a transversal vibration. The perceived sound was analyzed using "sound forge" software (for sound measurement).

For standardized tests of the impact insulation in a laboratory setting (ASTM 492), a machine with five steel-plated hammers was used as a source of noise shocks (ASTM E492 1996). The resulting value corresponded to the Impact Insulation Class (IIC), an integer-number indicating how well a building floor attenuates impact sounds such as footsteps.

3. Results and Discussion

3.1 Compressive and Tensile Strengths

The density of the tested binary ranged from 1375 to 1560 kg/m^3; the strength appears to decrease as the density increases. The drop in the compressive strength is more important than that of the tensile strength. This phenomenon is caused by the presence of the fines, which affect the microcracking behavior of the materials. A decrease in the amount of mixing water would partly mitigate this drop in strength and consequently improve the mechanical properties of the material because the water dosage is directly linked to the porosity of the concrete. When the density is about 1550 kg/m^3, scoria concrete plays an opposite role in the resistance compared with that of ordinary concretes.

In series A ternary concretes, there was a broad dispersion in the average compressive strength values for densities from 1408 to 1425 kg/m^3. The dispersion compared with the average value is 23% for the compressive strength and 1.5% for the tensile strength. These results were unexpected; the two plots of compressive and tensile strengths should have similar aspects, as the tested samples had nearly equal porosity values. It is thus concluded that the strengths are modified by a different size of aggregates based on the parameters considered in this study.

For series B ternary concretes, the porosity is more significant with coarse aggregates, which explains the drop in strength. The compressive strength thus decreases by 5% when the density of the concrete exceeds 1620 kg/m^3. This can be explained by the fact that the density of the scoria concrete must be less than 1600 kg/m^3 in order to obtain a structural and light insulating concrete (Shink and Alaiwa 2016).

Figure 4 shows the variation in the strength for series C ternary concretes according to density. There was an increase in the compressive strength as the density increases, with a maximum compressive strength of 22 MPa for a density of 1720 kg/m^3; after this point, the compressive strength decreases. The tensile strengths of the concretes are five times weaker than the compressive strengths. The variation depends on the cement dosage in the concrete (concrete density of 250–450 kg/m^3) from 4.39 to 21.92 MPa at 28 days.

Figure 5 shows the variation in the strengths of the binary concretes caused by the fraction of fines. An increase in fine fraction from 0.53 to 0.68 triggers reductions in both the compressive and tensile strengths. The smallest packing density of the granular arrangement results from the partial

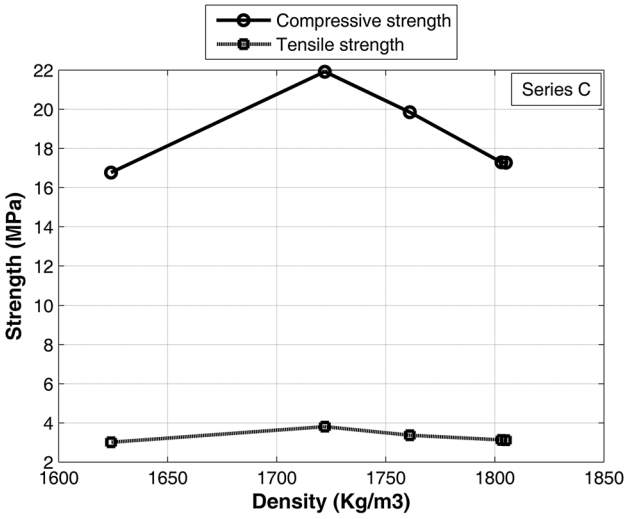

Fig. 4 Variation of strength of series C according to densities.

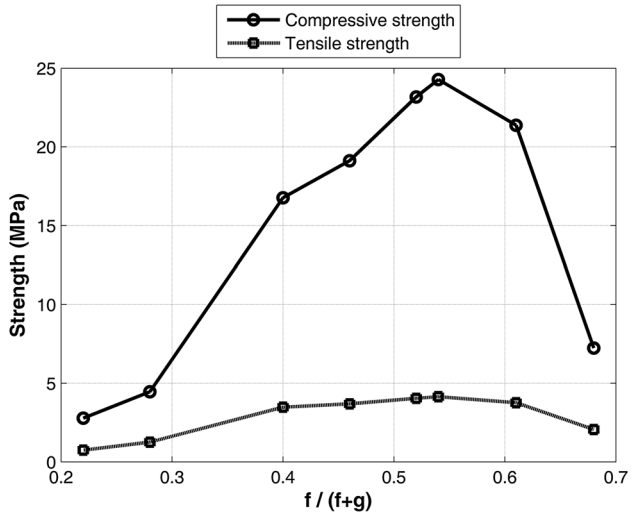

Fig. 5 Perturbation caused by the fines on the strength of binary concretes.

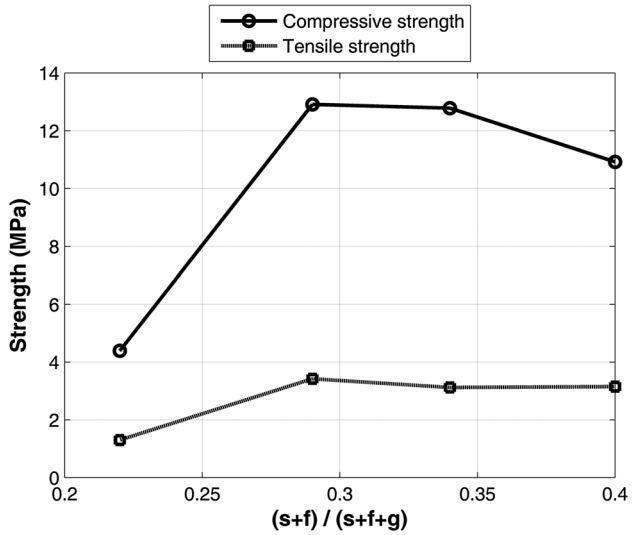

Fig. 6 Variation of strength of ternary concretes according to sand and fine content.

reduction in the fraction of coarse aggregates, which increases the porosity of the concrete.

The different size of the aggregates also affects the compressive strength of lightweight concretes in a linear pattern. The fragmentation of large aggregates occurs through the largest pores, which are thus eliminated. The positive influence of reducing the maximum sizes of the aggregate particles on the strength of concrete has been reported (Babu and Babu 2003). This phenomenon was also confirmed by Miled et al. (2007), who focused on polystyrene concrete and especially on concrete with low percentages of aggregates.

Figure 6 shows the variation in the strength of ternary concretes according to the sand and fine content levels. Initially, with increasing amounts of sand, the compressive and tensile strengths increase. Then, a progressive dispersion decrease occurs (Eq. 3) between the tensile and compressive strengths, with the ratio defined as follows (Bhattacharjee 2014):

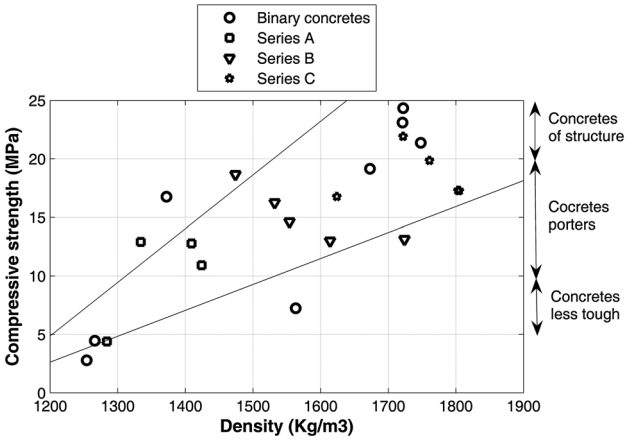

Fig. 7 Compressive strength as a function of densities.

$$r = \frac{s + f}{s + f + g} \tag{3}$$

where r is the dispersion ratio, and s, f, and g represent sand, fine aggregates, and coarse aggregates, respectively.

The fine presence among these aggregates can influence the relation between the densities and the mechanical properties of the concretes.

Figure 7 allows the definition of all possible different assignments based on the mass and strength of the concretes. Only the density values of concretes C3 and C4 are greater than 1800 kg/m^3. The density increases with the introduction of fines in the binary concretes and with the introduction of sand and fines in the ternary concretes. The water/cement (W/C) ratio has a significant impact on the hydrated cement paste because it influences the initial amount of space between the cement and the grains suspended in the mixing water (Chen and Brouwers 2007). Higher values of water/cement ratio correlate with more significant degrees of porosity (Baaroghel-Bouny et al. 2006). This triggers a decrease in the strength.

This type of construction material production is applied in almost all types of lightweight concretes and is used in many fields at a mechanical level. According to the classification by the American Concrete Institute (ACI 2003), there are highly resistant concretes (Rc >20 MPa) that can be used as structural materials, moderate-strength concrete with compressive strengths between 10 and 20 MPa that can be used as load-bearing elements, and low-strength concretes that can be used as beam filling for masonry. The impact of the thermal variation on the behavior of concretes is discussed below.

3.2 Thermal Analysis

3.2.1 Freeze–Thaw

Concretes bc1, bc2, and bc7 were able to resist the 400th freeze–thaw cycle. Paradoxically, the compressive strengths of concretes bc3, bc4, and bc8 peak between the 100th and 350th cycles. A weak permeability, arising from the absence of macroporosity and the highly efficient air bubble system, which is linked to the tortuosity network of the pores, disrupts the water movement (Cwirzen and Penttala 2005). The

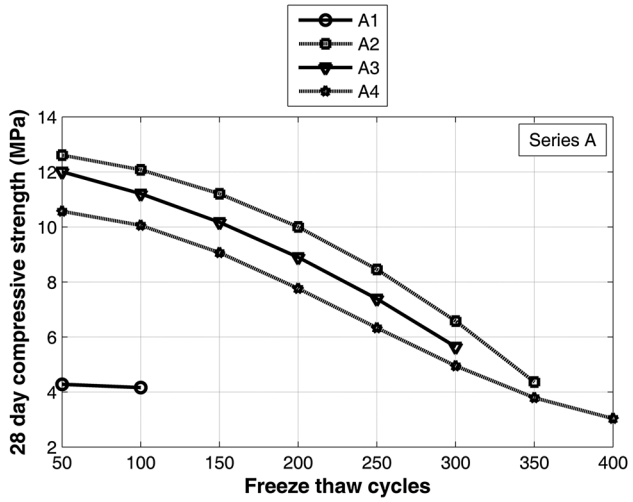

Fig. 8 Compressive strength at 28 days for series A during freeze thaw cycles.

fact remains that the tensile strength causes the destruction of concrete bc6 before the 50th freeze–thaw cycle.

In the absence of fines, the strengths of series A concretes drop to approximately 55% of the original strength in Fig. 8. This can be explained by the larger W/C ratio and sand percentage, which does not fill the voids in the large granules. From the 100th freeze–thaw cycle onward, all series B concretes decrease in strength. For concrete B5, the loss of compressive strength is approximately 62% before the 200th freeze–thaw cycle. Concretes B1 and B3, on the other hand, retain strength values equal to those measured while dry until the 400th cycle. This trend in strength can be explained by the pore structure, which governs the durability of the concrete, especially regarding the resistance of the concrete to freeze–thaw cycles (Sobolev and Batrakov 2007).

The analysis results of concretes C1 and C2 showed that the strength decreases more precipitously with freeze–thaw cycles when the fine percentage is equal to or greater than that of the cement. The fines create sites of weakness, which preferentially and more easily form cracks, so that microfissures are created by drying and not by frost.

Concretes C3, C4, and C5, having high sand proportions, have recorded decreases in strengths explained by their water content being high and quickly frozen. In addition to this effect, the moderate strength of these concretes does not allow the support of an increased volume, which was not constrained during the freeze–thaw cycles.

As summarized in Tables 6 and 7, the first 40 freeze–thaw cycles were conducted in order to obtain accurate results of the influence of the maximum size of the granules on the strength of the concretes. The evolution of the strength relating to the average granule size was reported to show a lack of air void on the concrete (Gao et al. 2006).

The scaling cumulated mass after the conclusion of 56 cycles, as reported in Table 8, was measured by the second method of freeze–thaw cycling. Of the six formulated concretes, the obtained scaling cumulated masses over 56 cycles only conform to the specifications for four formulations. The obtained values of concretes bc1 and bc2 are only slightly over the threshold.

The specifications were formed on the basis of concretes that were said to be resistant to scaling if the cumulated mass at the end of 56 cycles was less than or equal to 600 g per square meter of exposed surface area. Concrete bc6 was fully transformed into scales owing to the low cement proportion included in its composition.

3.2.2 Thermal Conductivity

The thermal conductivity measurement results are presented in Tables 9 and 10. According to these results, the thermal conductivity increases according to the amounts of sand and added binder material. In fact, the sand addition fills the pores created by large particles. Air, which is an excellent natural insulator, is replaced by thermally conductive binder materials. It is noted that the thermal conductivity increased when the amount of sand added to the cement is higher than that of water content.

The pore structure of a material plays a dominant role in controlling its thermal conductivity (Hilal et al. 2015). Hemp concrete, manufactured by a projection process, as shown by Elfordy et al. (2008), has a conductivity that can reach 0.49 W/m K for a volumetric mass of 550 kg/m^3. By comparison, hemp concrete is an excellent insulating material compared to pozzolan concrete, with a thermal conductivity value varying from 0.206 to 0.616 W/m K.

It is important to note the fundamental role of the porosity in the behavior of materials. In terms of the mechanical properties, the presence of air bubbles tends to make the material more fragile and limits the performance level. In terms of the thermal properties, the presence of air decreases the volumetric proportion of the material conducting the heat.

3.3 Acoustic Analysis

Generally, the absorption coefficient increases with the frequency up to 1 kHz. Concretes with low cement dosage rates absorb more sound at low frequencies, displaying the most interesting practical behavior. On the contrary, concretes with high dosage rates absorb more sound at higher

Table 6 Influence of coarse granulate dimension to the binary concretes on the compressive strength (in MPa) after 40 freeze thaw cycles.

D_{max} (mm)	Bc1	Bc2	Bc3	Bc4	Bc5	Bc7	Bc8
05	22.2	19.92	18.00	17.10	4.24	17.02	7.20
10	22.4	19.22	18.08	17.00	4.56	17.89	7.32
15	23.09	21.76	18.17	16.98	4.98	20.12	7.44

Table 7 Influence of coarse granulate dimension to the ternary concretes on the compressive strength (in MPa) after 40 freeze thaw cycles.

D_{max} (mm)	A				B					C				
No	1	2	3	4	1	2	3	4	5	1	2	3	4	5
05	3.90	12.22	9.31	10.42	18.76	16.22	14.38	9.43	10.75	21.45	19.79	16.66	16.92	16.52
10	3.91	12.27	10.81	10.43	18.79	16.30	14.45	11.12	12.40	21.52	19.82	16.85	17.06	16.68
15	3.92	12.51	12.52	10.52	19.00	16.32	14.87	12.02	13.23	21.65	19.89	17.22	17.13	16.91

Table 8 Scaling cumulated mass.

Name	Scaling cumulated mass after 56 cycles M (g/m^2)
bc1	392
bc2	515
bc3	1552
bc4	2113
bc5	2884
bc7	805
bc8	1017
A1	5075
A2	3115
A3	3160
A4	4415
B1	298
B2	844
B3	974
B4	2398
B5	3012
C1	618
C2	702
C3	1042
C4	4042
C5	4201

Table 9 Values of the thermal conductivity of the concretes without sand in W/m K.

Name	λa [W/m K]
bc1	0.402
bc2	0.394
bc3	0.381
bc4	0.309
bc5	0.268
bc6	0.206
bc7	0.330
bc8	0.288

frequencies. By comparing the absorption coefficients obtained from binary mixtures to those obtained from ternary series A concretes, it is concluded that the absorption coefficients are the lowest with the addition of fines at equal degrees of concrete porosity. Indeed, for low absolute void ratios (corresponding series A ternary concrete, with apparent densities of approximately 1400 kg/m^3), there was an increase in the absorption coefficient by approximately 50% at an intermediate frequency with a 350-kg/m^3 cement dosage in comparison with the coefficients obtained at a cement dosage of 300 kg/m^3.

For samples bc1, bc3, and bc7, the absorption levels are steady in all frequency ranges. Concretes at high dosages rates absorb intermediate and high sound frequencies, i.e., concretes bc4, bc5, bc6, A1, and A4, which may be used for acoustical corrections. The good sound absorption characteristics of these concretes at average and high frequencies are suitable for a reduction in the dominant frequencies of industrial noise.

The obtained absorption coefficient αmax is approximately 0.27 for concrete C1. In other words, about 27% of the sound is absorbed by the samples. A porous network consists of microbubbles. Therefore, auditory waves are reflected by the surface of the sample, which is not permeable, and cannot penetrate the material to be deadened. Concretes bc1, bc2, and B1 in Fig. 9 have absorption coefficients αmax ranging from 0.14 to 0.18. This may result from the more significant quantity of fines in the mixtures, which would make concretes bc1, bc2, and B1 even more impermeable than concrete C1.

Among lightweight concretes, only concrete using wood-made cement is currently used for its acoustical qualities. It absorbs more than 75% of the incident sonic wave energy at intermediate frequencies. Some materials such as bricks and shuttered concrete are not very permeable and do not let sound waves penetrate. Aerated concrete absorbs no more than 35% of the sound waves that intercept it. For scoria concretes with dosages equal to 350 kg/m^3, the absorption coefficients range from 0.32 to 0.44. These values are high compared to those of other building materials such as bricks

Table 10 Values of the thermal conductivity of the concretes with sand in W/m K.

Name	λa [W/m K]
A1	0.257
A2	0.299
A3	0.380
A4	0.385
B1	0.401
B2	0.452
B3	0.483
B4	0.524
B5	0.544
C1	0.421
C2	0.565
C3	0.616
C4	0.647
C5	0.657

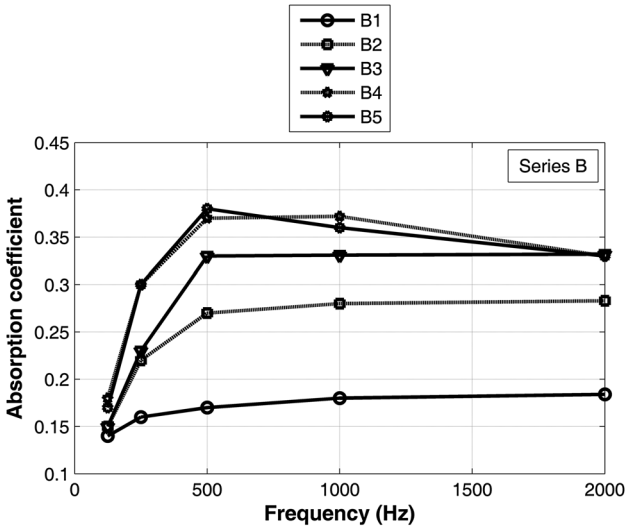

Fig. 9 Absorption coefficients of the ternary concretes of series B.

(from 0.03 to 0.05), shuttered concrete (from 0.01 to 0.02), and aerated concrete (from 0.23 to 0.32).

Housing insulation is seldom addressed despite its comfort-related properties. It is difficult to create two close plates without a rigid binder phase. Well-adapted plate systems of walls and floors are built and used as acoustical environments.Many complex systems have been proposed in the literature to improve the absorption of walls; for example, Zhang et al. (2000) proposed the use of MPPs with holes of different diameters to widen the absorption band of the MPP system. Ricardi (2001) also studied acoustical transmission through a rigid perforated screen backed with granular materials. A Kundt's tube was used to study the absorption

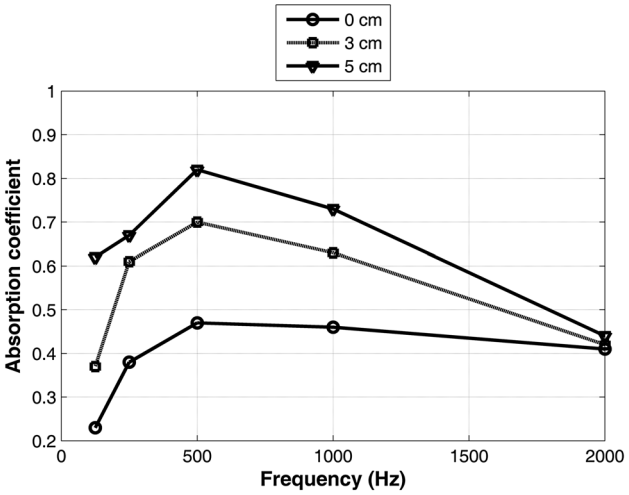

Fig. 10 Absorption coefficients of the concrete A1 with a certain air space.

coefficient of concrete A1. Between concrete A1 and the tube bottom, an air space of varying thickness exists. The results are shown in Fig. 10.

The absorption increases according to the air space thickness. However, at larger thicknesses, the degrees of increase are smaller. With these results, the tests were continued with the two concretes that exhibited the most absorption, ternary concrete A1 and binary concrete bc6, divided by an air space measuring approximately 5 cm. There was an increase in the absorption coefficient as the frequency increased, with a maximum absorption coefficient of 0.92 at a frequency of 500 Hz; after this point, absorption coefficient decreased until 0.37 at a frequency of 2000 Hz.

Notably, ternary concrete A1 placed behind binary concrete bc6 shows an improved absorption coefficient at both low and high frequencies. This multi-material method seems to provide significant sound absorption and improve the acoustical performance of the concretes.

In all frequency ranges, the scoria concrete shows a slight decrease in the absorption coefficient compared with the wood-made concrete. At low frequencies, the difference ranges from 3 to 5%; at intermediate frequencies, the absorption coefficients are nearly the same; and at high frequencies, the wood-made concrete is greater by 4–7%. The physical impacts within the lightweight scoria concretes merit consideration.

According to the amount of scoria used to make the testing plate, the acoustical drag is somewhat significant. The horizontal parts in Fig. 11 indicate that the coarse scorias form a network in which low-wavelength sounds are absorbed. Every time a sound wave meets an obstacle, part of the energy that it carries is absorbed by the obstacle. This systematic impact based energy loss explains the decrease in the transmitted sound. The maximum variation in α at a low frequency is 37%, and is about 47% for a frequency of 500 Hz. Higher void ratios correspond to an easier transmission of sound through the concretes.

At each frequency, for an intergranular void ratio equal to 0.5, α is between 0.14 and 0.36 with an average value of

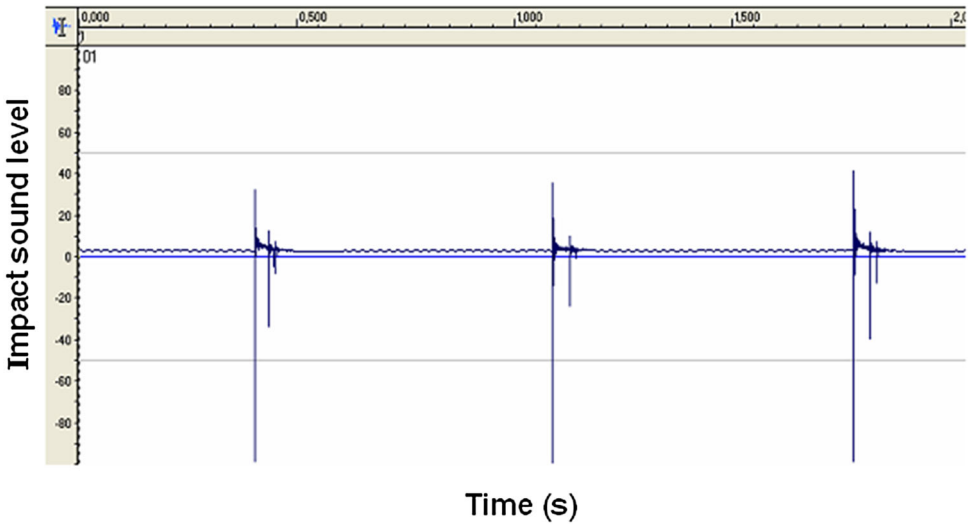

Fig. 11 Transversal vibration of the plate.

Table 11 Concretes classification according to their respective use.

Classification no	Compressive strength in 28 days	Thermal conductivity	Acoustic absorption coefficient (500 Hz)	Compressive strength after 300 freeze thaw cycles	Scaling cumulated mass after 56 cycles
1	bc2	bc6	A1	B1	B1
2	bc1	A1	A4	B3	bc1
3	C1	bc5	bc6	bc1	bc2
4	bc7	bc8	B5	bc7	C1
5	C2	A2	B4	bc2	C2
6	bc3	bc4	bc4	A4	bc7
7	B1	bc7	bc5	bc4	B2
8	C3	A3	B3	A2	B3
9	C4	bc3	C5	B2	bc8
10	C5	A4	C4	C4	C3
11	bc4	bc2	bc8	bc3	bc3
12	B2	B1	C2	C1	bc4
13	B3	bc1	B2	A3	B4
14	B5	C1	C3	C3	bc5
15	B4	B2	C1	B4	B5
16	A2	B3	A2	C2	A2
17	A3	B4	A3	C5	A3
18	A4	B5	B1	B5	C4
19	bc8	C2	bc2	bc8	C5
20	bc5	C3	bc3	A1	A4
21	A1	C4	bc1	bc5	A1
22	bc6	C5	bc7	bc6	bc6

approximately 0.25 ± 0.11. Acoustically, the intergranular voids have a real impact on the behavior of the concrete.

The physical characteristics of the size and density also affect the vibrational modes of the plate, which is reflected in the measured absorption coefficient. Coarse scoria constituents can be revised to reach the optimal compositions for lightweight concretes.

Concrete slab bc4 with a thickness of 150 mm covered with a 40-mm-thick layer of concrete bc2 exhibits an IIC value of ∼ 40; the same concrete slab with a 20-mm-thick layer of concrete A1 and a 20-mm-thick layer of concrete bc6 has an IIC value of more than 70. Harder concrete surfaces decrease the IIC value. Only a small gap exists between the IIC values measured with the concrete composed of the original scoria and that composed of the scoria mixed in water for 30 min. The IIC value reached 51 compared to the value of 50 for the reference. This small gap between the two indices can be explained by the weak acoustical escape induced by the grain structure.

In the light of this series of tests, it is possible to produce an optimal composition of scoria concrete for construction purposes based on the classifications given in Table 11.

4. Conclusion

Based on the average compressive strength after 28-day aging, thermal conductivity, acoustical absorption coefficient, expansion (stretch) after 300 freeze–thaw cycles without salts, and the scaling cumulated mass after 56 freeze–thaw cycles with salts, the following conclusions can be drawn for the studied materials and proportions:

- Low-resistance scoria concretes can be used in the domain of thermo–acoustical insulation;
- Ternary concretes placed behind binary concretes provide improvements in sound absorption on the order of 75% at low and intermediate frequencies. Thus, they can be used to weaken noise from a room to another or on both sides of a wall;
- By changing the average size of the large aggregate from 5 cm to 10 cm, the scoria concrete strength increases to 8% after 40 freeze–thaw cycles;
- The susceptibility to salt scaling of scoria concrete is not correlated with the susceptibility to internal frost action.
- Coarse scoria were used in two concrete samples of the same density of 450 kg/m^3. The average strength at 28 days was 14 MPa for the sample containing natural aggregates and 16.9 MPa for the soaked aggregates that had previously been mixed with water for 30 min. This represents a relative increase of approximately 20% over the strength of the reference concrete.
- The mixture of scoria in their original state and scorias mixed in water for 30 min led to an increase in the thermal conductivity by 5%. Simultaneously, the acoustical absorption coefficient was enhanced by a factor of 0.98–0.99.

Open Access

This article is distributed under the terms of the Creative Commons Attribution 4.0 International License (http://creativecommons.org/licenses/by/4.0/), which permits un restricted use, distribution, and reproduction in any medium, provided you give appropriate credit to the original author(s) and the source, provide a link to the Creative Commons license, and indicate if changes were made.

References

ACI (2003). *Guide for structural lightweight aggregate concrete* (p. 38), ACI 213R-03, ACI Committee 213, American Concrete Institute.

Al-Chaar, G.K., Alkadi, M., Yaksic, D.A., & Kallemeyn, L.A. (2011). *The use of natural pozzolan in concrete as an additive or substitute for cement*. ERDC/CERL TR-11-46.

Al-Swaidani, A. M., & Aliyan, S. D. (2015). Effect of adding scoria as cement replacement on durability-related properties. *International Journal of Concrete Structures and Materials, 9*(2), 241–254.

Asdrubali, F., & Pispola, G. (2007). Properties of transparent sound absorbing panels for use in noise barriers. *Journal of the Acoustical Society of America, 121*(1), 214–221.

ASTM E492 (1996). Standard test method for laboratory measurement of impact sound transmission through floor-ceiling assemblies using the tapping machine.

ASTM C117 (2004). Standard test method for materials finer than 75-μm (No. 200) sieve in mineral aggregates by washing.

ASTM C150 (2009). Standard specification for Portland cement. 10 pp. doi:10.1520/C0150_C0150M-09.

ASTM C 618 (2001). *Standard specification for coal fly ash and raw or calcined natural pozzolan for use as a mineral admixture in concrete*, ASTM C618-00, Annual Book ASTM Standard 04.02, 310-313.

ASTM C 33-03 (2003). *Standard specifications for concrete aggregates*.

ASTM C 143 (2014). Slump of hydraulic cement concrete. C. Roberts. doi:10.1520/C0143_C0143M-08. http://www.astm.org/cgi-bin/resolver.cgi?C143C143M-08.

ASTM International. (2009). *Annual book of ASTM standards*. West Conshohocken: ASTM International.

ASTM Standard C666/C666M-03(2003) (2008). Standard test method for resistance of concrete to rapid freezing and thawing. West Conshohocken: ASTM International. www.astm.org.

ASTM Standard C672. (1992). Standard test method for scaling resistance of concrete surfaces exposed to deicing chemicals. *American Society for Testing and Materials, Philadelphia, Annual Book of ASTM Standards, 04*(02), 341–343.

Baaroghel-Bouny, V., Mounanga, P., Khelidj, A., Loukili, A., & Rafal, N. (2006). Autogenous deformations of cement pastes: Part II. W/C effects, micro-macro correlations, and

threshold values. *Cement and Concrete Research, 36*(1), 123–136.

Babu, G. K., & Babu, S. D. (2003). Behaviour of lightweight expanded polystyrene concrete containing silica fume. *Cement and Concrete Research, 33*(5), 755–762.

Beaucour, A.L., Fiorio, B., & Ortola, S. (2003). Prediction of the elastic modulus of structural lightweight aggregate concrete. In: *Proceedings of the 6th CANMET/ACI International Conference on Recent Advances in Concrete Technologies*, Bucharest, Romania.

Bediako, M., Kevern, J., & Amankwah, E. (2015). Effect of curing environment on the strength properties of cement and cement extenders. *Materials Sciences and Applications, 6,* 33–39. doi:10.4236/msa.2015.61005.

Bessenouci, M.Z., Triki, N.E.B., Khelladi, S., Draoui, B., & Abene, A. (2011). The apparent thermal conductivity of pozzolana concrete. *Seventh International Conference on Material Sciences (CSM7)*, Beirut–Lebanon. Elsevier-Physics Procedia 21, 59–66.

Beycioğlu, A., Doğan D., Çullu, M., & Şamandar, A. (2010). Alkali Silika Reaksiyonu Ve Beton Durabilitesine Etkileri. MYO-ÖS- Ulusal Meslek Yüksekokulları Öğrenci Sempozyumu, 21-22 EKİM –DŰZCE.

Bhattacharjee, B. (2014). Concrete Technology. Department of Civil Engineering Indian Institute of Technology, Delhi. Aggregates, lecture – 07.

Bodet, R. (2014). Standards and regulations: Present status in France vs, Europe and other countries. Workshop ENPC "Recycling concrete into concrete".

Bondar, D. (2015). Sulfate resistance of alkali activated pozzolans. *International Journal of Concrete Structures and Materials, 9*(2), 145–158. doi:10.1007/s40069-014-0093-0.

Burlion, N., Bourgeois, F., & Shao, J. F. (2005). Effects of desiccation on mechanical behaviour of concrete. *Cement and Concrete Research, 27*(3), 367–379.

Chen, W., & Brouwers, H. J. H. (2007). The hydration of slag, part 2: Reaction models for blended cement. *Journal of Materials Sciences, 42*(2), 444–464.

Chen, B., & Liu, J. (2004). Properties of lightweight expanded polystyrene concrete reinforced with steel fiber. *Cement and Concrete Research, 4*(7), 1259–1263.

Chi, J. M., Huang, R., Yang, C. C., & Chang, J. J. (2003). Effect of aggregate properties on the strength and stiffness of lightweight concrete. *Cement & Concrete Composites, 25*(2), 197–205.

Coussy, O., & Fen-Chong, T. (2005). Crystallization, pore relaxation and microcryosuction in cohesive porous materials. *Comptes Rendus Mécanique, 333*(6), 507–512.

Coussy, O., & Monteiro, P. (2007). Unsaturated poroelasticity for crystallization in pores. *Computers and Geotechnics, 34*(4), 279–290.

Cwirzen, A., & Penttala, V. (2005). Aggregate-cement paste transition zone properties affecting the salt-frost damage of high-performance concretes. *Cement and Concrete Research, 35*(5), 671–679.

De Sa, C., Benboudjema, F., Duong, K., & Sicard, J. (2006). A meso-scale approach for the modeling of concrete behavior at high temperatures (pp. 557-564). In: *Proceedings of the Euro-C Conference on Computational Modelling of Concrete structures, Austria 2006.* The Netherlands: Taylor and Francis/Balkema.

de Sensale, G. R., & Goncalves, A. F. (2014). Effects of fine LWA and SAP as internal water curing agents. *International Journal of Concrete Structures and Materials, 8*(3), 229–238.

Durán-Herrera, A., Juárez, C. A., Valdez, P., & Bentz, D. P. (2011). Evaluation of sustainable high-volume fly ash concretes. *Cement & Concrete Composites, 33,* 39–45.

Elfordy, S., Lucas, F., Tancret, F., Scudeller, Y., & Goudet, L. (2008). Mechanical and thermal properties of lime and hemp concrete («hemprete») manufactured by a projection process. *Construction and Building Materials, 22*(10), 2116–2123.

Ezziane, K., Bougara, A., Kadri, A., Khelafi, H., & Kadri, E. (2007). Compressive strength of mortar containing naturel pozzolan under various curing temperature. *Cement & Concrete Composites, 29*(8), 587–593.

Gao, P., Wu, S., Lin, P., Wu, Z., & Tang, M. (2006). The characterisitics of air void and frost resisttance of RCC with fly ash and expansive agent. *Construction and Building Materials, 20*(8), 586–590.

Ghrici, M., Kenai, S., & Said-Mansour, M. (2007). Mechanical properties and durability of mortar and concrete containing natural pozzolana and limestone blended, cements. *Cement & Concrete Composites, 29*(7), 542–549.

Hamoush, S., Picornell-Darder, M., Abu-Lebdeh, T., & Mohamed, A. (2011). Freezing and thawing durability of very high strength concrete. *American Journal of Engineering and Applied Sciences, 4*(1), 42–51.

Hilal, A. A., Thom, N. H., & Dawson, A. R. (2015). The use of additives to enhance properties of pre-formed foamed concrete. *IACSIT International Journal of Engineering and Technology, 7*(4), 286.

ISO 354 (2003). Measurement of sound absorption in reverberation room, acoustics.

Kang, J., & Brocklesby, M. W. (2005). Feasibility of applying microperforated absorbers in acoustic window systems. *Applied Acoustics, 66*(6), 669–689.

Khedari, J., Charoenvai, S., & Hirunlabh, J. (2003). New insulating particleboards from durian peel and coconut coir. *Building and Environment, 38*(3), 435–441.

Lotfy, A., Hossain, K. M., & Lachemi, M. (2015). Lightweight self-consolidating concrete with expanded shale aggregates: Modelling and optimization. *International Journal of Concrete Structures and Materials, 9*(2), 185–206.

Maa, D. Y. (2007). Practical single MPP absorber. *International Journal of Acoustics and Vibration, 12*(1), 3–6.

Miled, K., Sab, K., & Le Roy, R. (2007). Particle size effect on EPS lightweight concrete compressive strength: Experimental investigation and modelling. *Mechanics of Materials, 39*(3), 222–240.

Mouli, M., & Khelafi, H. (2008). Performance characteristics of lightweight aggregate concrete containing naturel pozzolan. *Building and Environement, 43*(1), 31–36.

Norme NF EN 206-1 (2004). Concrete - Part 1: Specification, performance, production and conformity, AFNOR.

Parhizkar, T., Najimi, M., Pourkhorshidi, A. R., Jafarpour, F., Hillemeier, B., & Herr, R. (2010). Proposing a new approach for qualification of natural pozzolans. c Sharif University of Technology. Transaction A. *Civil Engineering, 17*(6), 450–456.

Penttala, V. (2006). Surface and internal deterioration due to saline and non-saline freeze thaw loads. *Cement and Concrete Research, 36*(5), 921–928.

Rabehi, B., Ghernouti, Y., & Driss, M. (2014). Potential use of calcined silt of dam as a pozzolan in blended Portland cement. *International Journal of Concrete Structures and Materials, 8*(3), 259–268. doi:10.1007/s40069-014-0072-5.

Ricardi, P. (2001). Study on the acoustic transmission loss of a rigid perforated screen backed with porous granular material. In: *Proceedings of 17th ICA*, Rome.

Rossignolo, J. A., Agnesini, M. V. C., & Morais, J. A. (2003). Properties of high- performance LWAC for precast structures with Brazilian lightweight concrete. *Cement and Concrete Composite, 25*(1), 77–82.

Ruzzene, M. (2004). Vibration and sound radiation of sandwich beams with honeycomb truss core. *Journal of Sound and Vibration, 277*(4–5), 741–763.

Shink, M., & Alaiwa, A. A. (2016). Structural lightweight concrete or mortar, method for manufacturing same and use thereof as self-placing concrete. US 2014/0336305 A1. 8 pp.

Sobolev, K. G., & Batrakov, V. G. (2007). Effect of a polyethylhydrosiloxane admixture on the durability of concrete with supplementary cementitious materials. *Journal of Materials in Civil Engineering, 19*(10), 809–819.

UCGCT (2009). Understanding cement glossary of cementitious terms, Version 2.5, © WHD Microanalysis Consultants Ltd.

UNESCO. (1995). *Major regional project geology for sustainable development* (pp. 0258–3674). Paris: UNESCO.

Valenza, J. J., II, & Scherer, G. W. (2007). A review of salt scaling: I. Phenomenology. *Cement and Concrete Research, 37*(7), 1007–1021.

Vlček, J., Drongová, L., Topinková, M., Matějka, V., Kukutschová, J., Vavro, M., et al. (2014). Identification of phase composition of binders from alkali activated mixtures of granulated blast furnace slag and fly ash. *Ceramics – Silikáty, 58*(1), 79–88.

XPP 18420, (1995). Concrete- test on scaling surfaces of hardened concrete exposed to frost in presence salt solution. AFNOR.

Yaşar, E., Atis, C. D., & Kiliç, A. (2004). High strength lightweight concrete made with ternary mixtures of cement-fly ash-silica fume and scoria as aggregate. *Turkish Journal of Engineering and Environmental Sciences, 28,* 95–100.

Zhang, B., Lang, Ge, S.P., & Zhuang, W. (2000). The study of sound absorption characteristic of micro-perforated panel with different diameter holes (p. 3871-3874). In *Proceedings of Internoise-2000.* France: Nice.